—研究論文—
Scientific Papers

Magnetic Analysis of an Antarctic Mesosiderite, ALH-77219

Takesi NAGATA* and Minoru FUNAKI*

南極隕石 ALH-77219 メソシデライトの磁気分析

永田　武*・舟木　實*

要旨: 南極隕石のコレクションのうちでは稀少な，メソシデライト ALH-77219 の磁気分析を行い，また，その中に含まれる金属粒の化学成分について，EPMA による分析を行った．EPMA 分析の結果，ALH-77219 中の金属相は，Ni 含有量 5–6 wt% のカマサイトおよび Ni 含有量約 50 wt% のテーナイト相とに 2 分される．ALH-77219 の熱磁化曲線は，平均 Ni 含有量 6 wt% のカマサイトと平均 Ni 含有量 54 wt% のテーナイトが混在し，そのテーナイト相の大部分は，テトラテーナイト規則格子構造を持つことを示す．6% Ni カマサイトおよび 54% Ni テーナイトの含有量は，それぞれ 19.3 wt% および 6.3 wt% である．

Abstract: Magnetic analyses are made on an Antarctic mesosiderite ALH-77219, and chemical analyses of metallic grains in the mesosiderite are carried out with the aid of an EPMA. The EPMA analyses show that the metallic phases in ALH-77219 are composed of kamacite of 5–6 wt% Ni and taenite of about 50 wt% Ni. The thermomagnetic analyses show that the mesosiderite ALH-77219 contains kamacite phase of about 6 wt% Ni on average of 19.3% in weight and taenite phase of about 54 wt% Ni on average of 6.3% in weight. The major parts of the taenite phase are of the superlattice structure of tetrataenite, which has a large magnetic anisotropy.

1. Introduction and Outline of Petrology of ALH-77219

The basic magnetic properties of mesosiderites (pyroxene-plagioclase stony-iron meteorites) have not yet been described in detail up to date. An Antarctic meteorite, ALH-77219, is identified as a mesosiderite (AGOSTO *et al.*, 1980; MASON, 1981). According to these previous works, ALH-77219 is a mesosiderite containing about 50% pyroxene, 20% metal and 15% fine grained matrix.

The ferromagnetic metallic minerals in ALH-77219 mesosiderite have been analyzed and studied in fair detail by AGOSTO *et al.* (1980), who have shown that the bulk of the metal is kamacite containing about 6% Ni and the remaining metallic parts are cloudy taenite, tetrataenite and schreibersite, and that metallic iron and nickel contents of the bulk chemical composition of ALH-77219 are 29.83 wt% and 8.7wt% respectively. They further reported that tetrataenite in ALH-77219 contains 47–54 wt% Ni, 0–0.05 wt% Co and 0.10–0.16 wt% Cu. In results of mineralogical studies of metallic

* 国立極地研究所. National Institute of Polar Research, 9–10, Kaga 1-chome, Itabashi-ku, Tokyo 173.

grains in ALH-77219 by AGOSTO *et al.* (1980), the tetrataenite phase takes place between kamacite and cloudy taenite forming the well-known M-shape distribution of Ni, or between schreibersite and kamacite.

As already experimentally demonstrated and discussed (NAGATA and FUNAKI, 1982), the magnetic properties of meteorites containing tetrataenite as one of major ferromagnetic constituents are characterized by a very high magnetic coercivity which is caused by a high magnetic anisotropy of the tetrataenite phase. One of the main aims of the present study is therefore a magnetic examination of ALH-77219 containing a considerable amount of tetrataenite, mineralogical and chemical structures of which have been fairly well studied. In addition, a general description of the magnetic properties of a mesosiderite will be another contribution to the magnetic classification scheme of meteorites.

Since mineralogical and chemical compositions of a meteorite are not exactly homogeneous but considerably heterogeneous in many cases, mineralogical and chemical compositions of metallic grains in several parts of an ALH-77219 sample which is magneti-

Table 1. Chemical composition of typical metallic grains in ALH-77219 mesosiderite.

(1) Grain (I)

Element	Kamacite phase (wt%)					Taenite phase (wt%)		
	1	2	3	4		1	2	3
Fe	92.10	94.55	91.44	94.00	Boundary	50.74	60.85	58.67
Ni	4.65	5.31	5.49	4.65		49.33	34.78	40.44
Co	0.54	0.76	0.67	0.52		0.20	0.09	0.15
S	0.00	0.00	0.03	0.01		0.02	0.02	0.00
Total	97.29	100.62	97.63	99.18		100.29	95.74	99.26

(2) Grain (II)

Element	Kamacite phase (wt%)							Taenite phase (wt%)		
	1	2	3	4	5	6		1	2	3
Fe	94.07	92.94	94.82	93.84	93.31	94.55	Boundary	49.97	50.83	48.39
Ni	4.60	5.80	6.21	6.25	6.24	5.71		50.58	48.44	48.61
Co	0.64	0.67	0.58	0.65	0.62	0.59		0.14	0.14	0.27
S	0.02	0.00	0.01	0.06	0.00	0.00		0.00	0.02	0.004
Total	99.33	99.41	101.62	100.80	100.17	100.85		100.69	99.43	97.274

(3) Grain (III)

Element	Kamacite phase (wt%)			Tetrataenite phase (wt%)		Cloudy taenite phase (wt%)	
	1	2	3	1	2	1	2
Fe	90.83	92.63	92.49	51.02	51.42	53.15	56.69
Ni	4.57	4.80	4.97	48.14	46.53	44.16	41.03
Co	0.43	0.41	0.29	0.08	0.11	0.18	0.06
S	0.07	0.02	0.00	0.03	0.01	0.03	0.00
Total	95.90	97.86	97.75	99.27	98.07	97.52	97.78

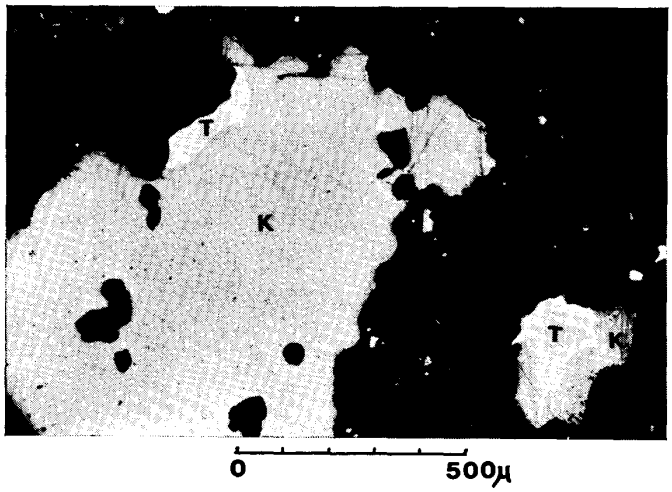

Fig. 1a. Metallic grains in ALH-77219 mesosiderite. Grain I; a larger grain on the left. Grain II; a smaller grain on the right. K; kamacite. T; taenite. In addition to the two large grains comprising kamacite and taenite phases, a number of small grains of Fe-Ni metal (white spots) are distributed in the matrix.

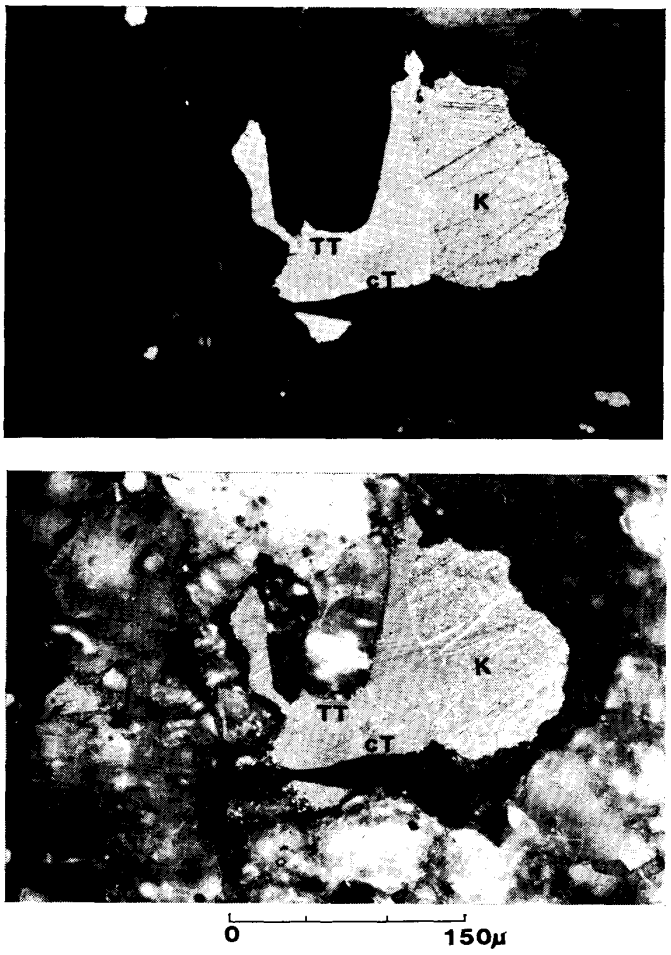

Fig. 1b. Metallic grain (III) in ALH-77219 mesosiderite. Top; etched surface. Bottom; the same surface under crossed polars. K; kamacite. TT; tetrataenite. cT; cloudy taenite.

cally analyzed in the present study are examined in order to directly compare the magnetic properties with the ferromagnetic mineralogical composition in a same meteoritic specimen. As shown in Fig. 1, for example, the metallic component in the ALH-77219 mesosiderite consists mostly of kamacite and taenite. The chemical composition of kamacite and taenite phases in metallic grains I and II shown in Fig. 1a are measured by an EPMA, results being summarized in Table 1, where contents of Fe, Ni, Co and S are measured at each point along a straight line crossing both kamacite and taenite phases. As given in Table 1, Ni and Co contents in the kamacite phase are 5–6 wt% and 0.5–0.7 wt% respectively, while those in the taenite phase are 40–50 wt% and 0.1–0.3 wt% respectively.

In metallic grain I, Site 1 through 4 in the kamacite phase are distributed along a straight line from the outer edge of kamacite phase toward the boundary between kamacite and taenite, while Site 1, 2 and 3 in the taenite phase are distributed from the boundary toward the outer edge of taenite phase (see Fig. 1a). In metallic grain II, the distribution order of measured points in the kamacite phase in from Site 1 near the outer edge of kamacite to Site 6 near the boundary between kamacite and taenite, while in the taenite phase Site 1 is near the boundary and Site 3 is located near the outer edge of taenite (see Fig. 1a). In both metallic grains, the chemical composition of taenite near the boundary in close to 50% Fe 50% Ni in atomic ratio, and it seems highly possible that the taenite phase very near the boundary is of the structure of tetrataenite.

Actually, the characteristic optical anisotropy of tetrataenite (CLARKE and SCOTT, 1980) is observed in metallic grain III shown in Fig. 1b, where the top photograph shows the etched surface of metallic grain III and the bottom one the same surface under crossed polars. In metallic grain III, a kamacite phase (K) is directly neighboured by a tetrataenite phase (TT) which envelops a cloudy taenite phase (CT). Chemical compositions of 3 points in K-phase, 2 points each in TT- and CT-phases distributed along a straight line are summarized in Table 1. The distributions of Ni and Co along a straight line passing through K, TT and CT phases in order of metallic grain III are similar to those of kamacite-taenite grains reported by AGOSTO *et al.* (1980). A similar tendency can be observed in metallic grain I too. No schreibersite is detected in the present sample of ALH-77219, but a possible presence of schreibersite-taenite grain cannot be rejected, because the mineralogical and chemical examinations are made only on random selected metallic grains.

2. Magnetic Hysteresis Characteristics

The basic magnetic parameters at room temperature (20°C), such as the saturation magnetization (I_S), the saturated isothermal remanent magnetization (I_R), the coercive force (H_C) and the remanence coercive force (H_{RC}), of a bulk specimen of ALH-77219 mesosiderite before heating and after twice heating up to 870°C in 1×10^{-4} torr atmosphere are summarized in Table 2.

As shown in Table 2, I_R, H_C and H_{RC} after the heating procedure have considerably decreased compared with their respectively corresponding values before the heating procedure, though I_S is maintained almost constant. Figure 2 shows the magnetization curves at 20°C of ALH-77219 sample before and after the heating procedure. It is

Table 2. Magnetic hysteresis and thermomagnetic characteristics of ALH-77219.

Magnetic parameters	Before heating	After heating	Unit
I_S	47.1	48.0	emu/g
I_R	0.688	0.532	emu/g
H_C	46	16.5	Oe
H_{RC}	520	137	Oe
Θ	560	560, 570	°C
$\Theta^*_{\alpha\to\gamma}$	759	759	°C
$\Theta^*_{\gamma\to\alpha}$	630	630	°C

Remarks
I_S : Saturation magnetization
I_R : Saturated isothermal remanent magnetization
H_C : Coercive force
H_{RC} : Remanence coercive force
Θ : Curie point of taenite
$\Theta^*_{\alpha\to\gamma}$: $\alpha\to\gamma$ transition temperature of kamacite
$\Theta^*_{\gamma\to\alpha}$: $\gamma\to\alpha$ transition temperature of kamacite

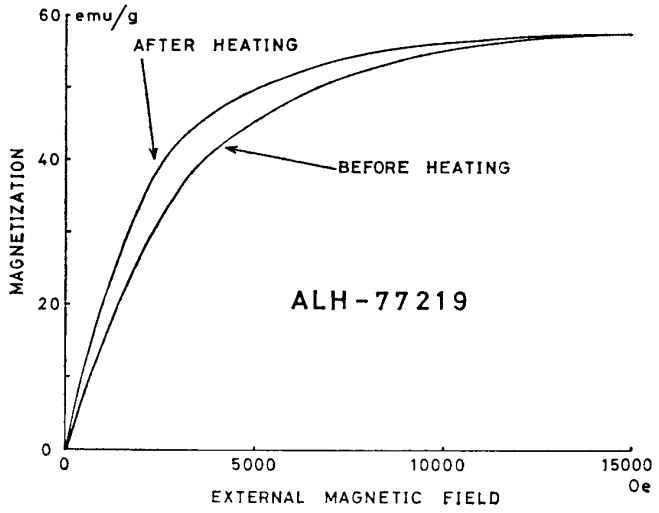

Fig. 2. Magnetization curves of Antarctic mesosiderite ALH-77219 at 20°C before and after heating to 870°C in 10^{-4} torr atmosphere.

shown in Fig. 2 that the magnetization after the heating procedure has become considerably softer than that before the heating procedure. These observed facts suggest that an original magnetic phase having a large magnetic coercivity and a large magnetic anisotropy has changed to a different magnetic phase which has smaller magnetic coercivity and anisotropy by the heat treatment. The I_S-value of ALH-77219 (I_S=47.1 emu/g) indicates that the content of iron-nickel metal is at least about 20 wt%.

3. Thermomagnetic Characteristics

Figures 3a and 3b illustrate the thermomagnetic curves of the first and the second

runs of ALH-77219, which were measured by a vibration magnetometer in 6000 Oe in external magnetic field and in 1×10^{-4} torr atmosphere. The magnetic transition at 759°C in the heating thermomagnetic curves of both the first and second runs can be identified as the $\alpha\rightarrow\gamma$ transition of kamacite, while the magnetic transition at 630°C in the cooling thermomagnetic curves gives the $\gamma\rightarrow\alpha$ transition of kamacite. These observed values of $\alpha\rightarrow\gamma$ and $\gamma\rightarrow\alpha$ transitions indicate that the Ni-content in the kamacite phase is approximately 6 wt% on average.

In the heating thermomagnetic curve of the first run, a sharp magnetic transition is detected at 560°C, and a less distinct transition point is detected at the same temperature on the cooling thermomagnetic curve. In the second-run thermomagnetic curves also, a sharp transition takes place at 570°C on the heating process and a less distinct transition occurs at 560°C on the cooling process. The cooling thermomagnetic curve of the second run is practically identical to that of the first run, as illustrated in the left diagram of Fig. 4. It may thus be concluded that these magnetic transition points essentially present a Curie point of taenite phase around 560°C, which indicates that the Ni-content in the taenite phase is about 54 wt% at maximum.

In comparing the second-run thermomagnetic curves in Fig. 3b with the first-run curves in Fig. 3a, the second-run cooling curve (II) is almost same as the first-run cooling curve (I), while the second-run heating curve (II) also is approximately same as the first-run heating curve (I) in a temperature range above 560°C. Thus, we may consider that the thermally irreversible thermomagnetic curves of the kamacite phase are not changed throughout the first- and second-run measurements. However, the second-run heating curve (II) is markedly different from the first-run heating curve (I) in a temperature range below 560°C. The first-run heating curve magnetization is characteristically flat and weak with an increase in temperature in comparison with the second-

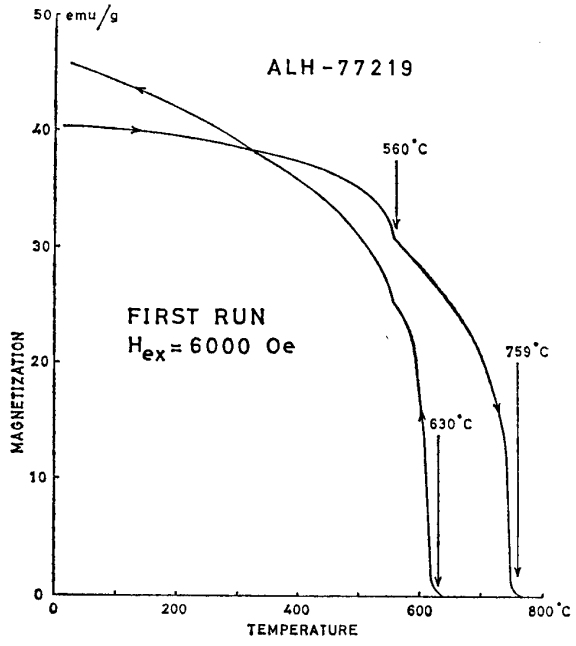

Fig. 3a. Thermomagnetic curve of ALH-77219 mesosiderite for the first-run heating and cooling cycle.

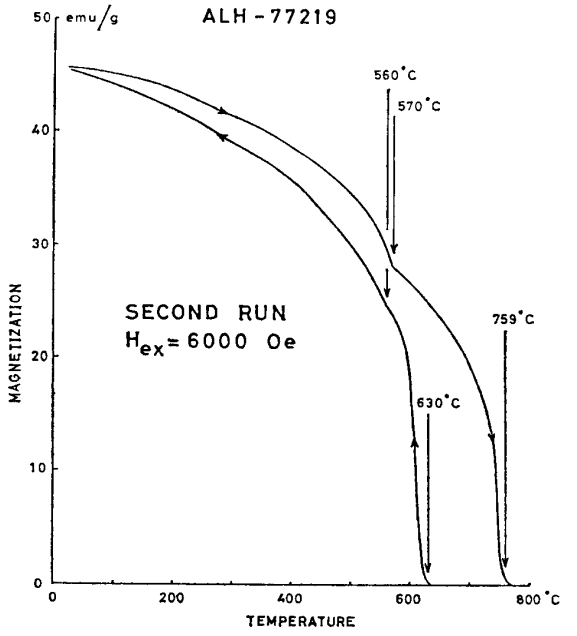

Fig. 3b. Thermomagnetic curve of ALH-77219 mesosiderite for the second-run heating and cooling cycle.

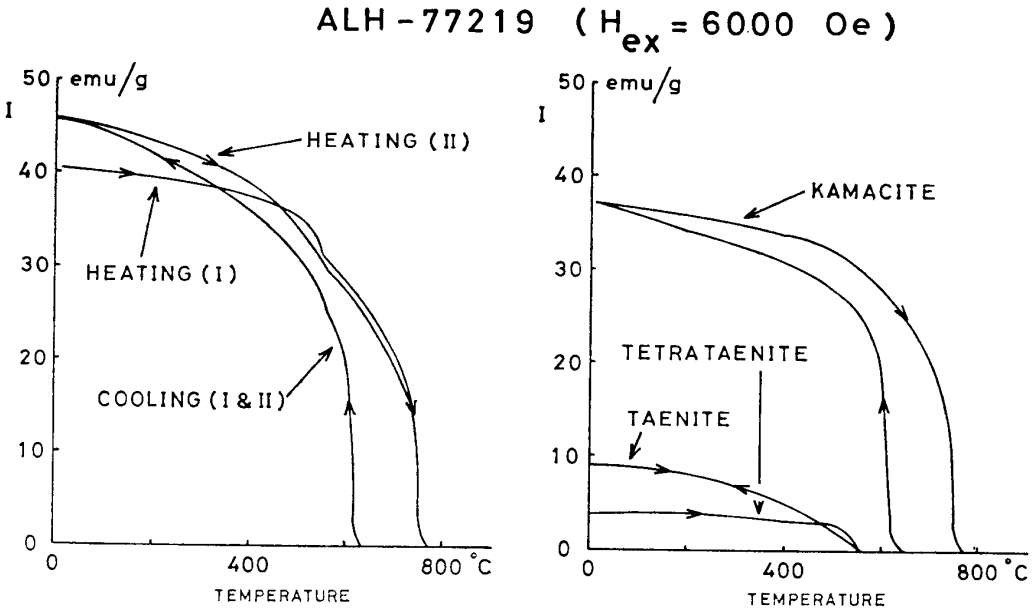

Fig. 4. Analysis of thermomagnetic curves of ALH-77219 mesosiderite. (Left) Observed first- and second-run thermomagnetic curves. (Right) Decomposed components of kamacite and taenite phase.

run heating curve in the temperature range. The shape of a thermomagnetic curve that is essentially flat up to about 500°C and then abruptly drops to Curie point is a typical characteristic of tetrataenite, when its magnetization is measured in a relatively weak magnetic field (*i.e.* smaller than 10 kOe), as demonstrated in tetrataenite-rich meteorites (NAGATA and FUNAKI, 1982; WASILEWSKI, 1982). We may then be able to interpret the heating thermomagnetic curve characteristics as that the magnetization of tetrataenite phase takes place only in the first-run curve in a temperature range below 560°C, and the tetrataenite phase has been transformed to the ordinary taenite by heating to 870°C. The thermally reversible thermomagnetic curve of the transformed ordinary taenite phase comes out in the second-run heating curve as well as in the first- and second-run cooling curves. In microscopic and EPMA studies of metallic grains by both AGOSTO *et al.* (1980) and the present authors, cloudy taenite phases have been clearly observed in addition to kamacite and tetrataenite phases. In the thermomagnetic curves shown in Fig. 3, however, the cloudy taenite phase and the tetrataenite phase are not clearly distinguishable from each other. If, for example, a considerable amount of cloudy taenite of 40 wt% Ni is contained in metallic grains, and if the cloudy taenite phase has a homogeneous chemical composition, it should have a distinctly defined Curie point at 360°C on the thermomagnetic curve. Such a magnetic transition point as expected in the above discussion cannot be detected in the observed thermomagnetic curves. As discussed later, it seems most likely that the cloudy taenite phase comprises, in its microstructure, a component of about 50 wt% Ni and the other component of less than 30 wt% Ni which is paramagnetic at room temperature (*e.g.* NAGATA and FUNAKI, 1982). Even if so, however, it may be difficult to determine whether the taenite phase of about 50 wt% Ni is of the ordinary f.c.c. cubic structure (ordinary taenite) or of the tetragonal structure (tetrataenite). We may assume in the present study, therefore, that the hypothetical component of taenite of about 50 wt% Ni is tetrataenite

or the amount of this component in cloudy taenite is negligibly small compared with the amounts of kamacite and tetrataenite phases, because no considerable evidence of presence of cloudy taenite is observed in the thermomagnetic curves. As far as the observed thermomagnetic curves are concerned, further, no trace of Curie point of schreibersite (lower than 400°C) can be detected, so that a possible schreibersite magnetization can be ignored in the present analysis.

Noting then the magnetization intensities at temperature T of tetrataenite, ordinary taenite, kamacite in the heating process and kamacite in the cooling process by $I_{tt}(T)$, $I_t(T)$, $I_k^{(h)}(T)$ and $I_k^{(c)}(T)$ respectively, the thermomagnetic curves of the first-run heating (Heating (I)), the second-run heating (Heating (II)), the first-run cooling (Cooling (I)) and the second-run cooling (Cooling (II)) can be approximately expressed as

$$\left.\begin{aligned} &[\text{Heating (I)}]=I_{tt}(T)+I_k^{(h)}(T),\\ &[\text{Cooling (I)}]=I_t(T)+I_k^{(c)}(T),\\ &[\text{Heating (II)}]=I_t(T)+I_k^{(h)}(T),\\ &[\text{Cooling (II)}]=I_t(T)+I_k^{(c)}(T). \end{aligned}\right\} \qquad (1)$$

This model can give rise to [Cooling (I)]=[Cooling (II)], [Heating (II)]−[Heating (I)]=$I_t(T)-I_{tt}(T)$, [Heating (II)]−[Cooling (II)]=$I_k^{(h)}(T)-I_k^{(c)}(T)$. In addition to the composition model expressed by (1), we may further make a reasonable assumption for general characteristics of a thermomagnetic curve of respective single phase ferromagnetic materials, such as

$$\left.\begin{aligned} &\frac{\partial I_{tt}(T)}{\partial T}\leqq 0, \quad \frac{\partial I_t(T)}{\partial t}\leqq 0, \quad \frac{\partial I_k^{(h)}}{\partial T}\leqq 0, \quad \frac{\partial I_k^{(c)}}{\partial T}\leqq 0,\\ &\frac{\partial^2 I_{tt}(T)}{\partial T^2}\leqq 0, \quad \frac{\partial^2 I_t(T)}{\partial T^2}\leqq 0, \quad \frac{\partial^2 I_k^{(h)}}{\partial T^2}\leqq 0, \quad \frac{\partial^2 I_k^{(c)}}{\partial T^2}\leqq 0. \end{aligned}\right\} \qquad (2)$$

With the aid of necessary conditions given by (1) and (2), thermomagnetic curves of individual components, $I_{tt}(T)$, $I_t(T)$, $I_k^{(h)}(T)$ and $I_k^{(c)}(T)$, can be approximately determined by analyzing the measured thermomagnetic curves, [Heating (I)], [Heating (II)] and [Cooling (I) and (II)]. The right-side diagram of Fig. 4 shows the three thermomagnetic curves of I_{tt} (Tetrataenite), I_t (Taenite) and a set of $I_k^{(h)}$ and $I_k^{(c)}$ (Kamacite) in ALH-77219 mesosiderite thus obtained by the analysis. It must be noted that the magnetization intensities of $I_{tt}(20°C)=3.9$ emu/g, $I_t(20°C)=9.0$ emu/g, and $I_k(20°C)=36.5$ emu/g shown in Fig. 4 are those measured in an external magnetics field of 6 kOe. In an external magnetic field of 6 kOe, I_t and I_k are approximately 90% of their saturation values as shown in Fig. 2. Since the saturation magnetization of kamacite of 6 wt% Ni is about 210 emu/g and that of ordinary kamacite of 54 wt% Ni is 160 emu/g (CRANGLE and HALLAM, 1963), the content of 6 wt% Ni kamacite and 54 wt% Ni taenite in ALH-77219 are estimated as 19.3 wt% and 6.3 wt% respectively.

Figure 3 further suggests that almost all original taenites are of the structure of tetrataenite, and these tetrataenite grains are almost completely transformed to the ordinary taenite by heating up to 870°C. It may thus be concluded that about a quarter in weight of ALH-77219 is occupied by iron-nickel metallic grains, and about a quarter in weight of the metallic component is tetrataenite of 54 wt% Ni and the remaining three quarters are kamacite of 6 wt% Ni.

4. Magnetic Characteristics of Tetrataenite Phase

It will be certain that the ferromagnetic phase having Curie point at about 560°C is taenite whose Ni-content is 54 wt% at maximum. As shown in Fig. 4, the first-run heating thermomagnetic curve of the tetrataenite phase in ALH-77219 is characterized by a very small decrease of magnetization with an increase of temperature up to about 500°C and then an abrupt decrease of magnetization down to Curie point above 500°C. In contrast to the tetrataenite thermomagnetic curve, the reversible thermomagnetic curve of ordinary taenite shown in Fig. 4 is satisfactorily similar to a saturated thermomagnetic curve of ordinary 50%Fe–50% Ni alloy (*e.g.* BOZORTH, 1951), and the magnetization intensity at room temperature of ordinary taenite is about 2.5 times as large as that of tetrataenite in an external magnetic field of 6 kOe.

It has already been shown (NAGATA and FUNAKI, 1982) that the thermomagnetic curve of tetrataenite in an external magnetic field of about 5 kOe is reduced in intensity to 1/2–1/3 of the ordinary-taenite magnetization of the same chemical composition and the decreasing gradient of magnetization with increasing temperature becomes considerably smaller than that of the ordinary taenite, because of the conspicuous magnetic anisotropy of tetrataenite and the effect of demagnetizing factor of taenite grains. The same characteristics of tetrataenite thermomagnetic curve have been pointed out in Yamato-74160 (LL7), ALH-77260 (L3) and St. Séverin (LL6) chondrites (NAGATA and FUNAKI, 1982) and in Appley Bridge amphotelite (WASILEWSKI, 1982), which all contain a considerable amount of tetrataenite.

A characteristic behaviour of the thermomagnetic curves of taenite and tetrataenite phases observed throughout these five examples including ALH-77219 is that the heating thermomagnetic curve of tetrataenite crosses that of ordinary taenite around 500°C or at a lower temperature, the tetrataenite magnetization becoming larger than the ordinary-taenite magnetization above 500°C. This characteristic behaviour can not be explained by the interpretation model of a structure transformation of the largely anisotropic tetrataenite to the almost isotropic taenite of a single chemical composition under the effect of a demagnetizing factor of concerned metallic grains.

In the case of St. Séverin (LL6) chondrite, coexistence of ordinary taenite of 25–30 wt% Ni, which is paramagnetic at temperature above 0°C, is detected by a Mössbauer analysis, and its cooling thermomagnetic curve indicates that tetrataenite domains are homogenized with ordinary-taenite matrix in various ratios by heating up to 800°C, resulting in various phases of ordinary taenites of different Ni-contents in a range of 30–50 wt% Ni (NAGATA and FUNAKI, 1982). It seems likely that tetrataenite grains in other meteorites also are associated with a small amount of taenite of less than 30 wt% in Ni-content. By heating to a high temperature, the tetrataenite grains may be homogenized with the surrounding low nickel taenite, resulting in ordinary-taenite phases of different values of Ni-content which have Curie points at temperatures lower than 560°C. Thus, one of the observed features that the magnetization intensity of tetrataenite is larger than that of the transformed ordinary taenite within a certain temperature range (down to about 500°C in the case of Fig. 4) below Curie point of tetrataenite could be reasonably interpreted.

This paper is a supplementary note to the authors' previous paper, "Magnetic properties of tetrataenite-rich stony meteorites" (NAGATA and FUNAKI, 1982). The authors' thanks are due to Dr. Roy CLARKE, Jr. who suggested them about metallographic characteristics of the metallic grains of ALH-77219 mesosiderite.

References

AGOSTO, W. A., HEWINS, R. H. and CLARKE, R. S., Jr. (1980): Allan Hills A77219, the first Antarctic mesosiderite. Proc. Lunar Planet. Sci. Conf. 11th, 1027–1045.

BOZORTH, R. M. (1951): Ferromagnetism. Princeton, D. van Nostrand, 112.

CLARKE, R. S., Jr. and SCOTT, E. R. D. (1980): Tetrataenite–ordered FeNi, a new mineral in meteorites. Am. Mineral., **65**, 624–630.

CRANGLE, J. and HALLAM, G. C. (1963): The magnetism of face-centered cubic and body-centered cubic iron-nickel alloys. Proc. R. Soc. London, Ser. A, **272**, 119–132.

MASON, B. (1981): ALHA-77219, Petrographic description, Antarctic meteorite descriptions, 1976–1977–1978–1979. Antarct. Meteorite Newslett., **4** (1), 37.

NAGATA, T. and FUNAKI, M. (1982): Magnetic properties of tetrataenite-rich stony meteorites. Mem. Natl Inst. Polar Res., Spec. Issue, **25**, 222–250.

WASILEWSKI, P. J. (1982): Magnetic characterization of tetrataenite and its role in the magnetization of meteorite (abstract). Lunar and Planetary Science XIII. Houston, Lunar Planet. Inst., 843–844.

(*Received March 7, 1983*)